metals

MDPI

Article

Development of Ultrafine Grain IF Steel via Differential Speed Rolling Technique

Young Gun Ko [1,*] and Kotiba Hamad [2,*]

[1] School of Materials Science and Engineering, Yeungnam University, Gyeongsan 38541, Korea
[2] School of Advanced Materials Science & Engineering, Sungkyunkwan University, Suwon 16419, Korea
* Correspondence: younggun@ynu.ac.kr (Y.G.K.); hamad82@skku.edu (K.H.)

Abstract: The aim of this paper was to investigate the microstructural development and properties of interstitial free (IF) steel fabricated using the DSR (differential speed rolling) process. Severe plastic deformation of the DSR passes was imposed on the sample for up to four passes, leading to ~1.7 total strain with a speed ratio of 1:4 between the two rolls. Microstructural observation revealed that the equiaxed grain size of ~0.7 μm, including the formation of grain boundaries with a high angle of misorientation, was reached after four operations of DSR, which was attributed to the grain subdivision of severely elongated ferrite grain. Since the deformation mode of the DSR operation was dominated by severe shear deformation, the main shear texture of the bcc components appeared in all DSR operations in which the α-fiber of the {110} slip became a main component in accommodating the severe plastic deformation of the DSR process. The intensity of the shear texture, the {110} and {112} slip, increased by increasing the number of passes. Moreover, the γ-fiber of the <112>-type planes was activated as a result of the alternation of the shear direction during sample rotation. The microhardness and room temperature tensile tests revealed that the strength of the IF steel improved as the amount of strain increased, and this was attributed to the grain refinement and texture characteristics of the samples after the DSR processing.

Keywords: severe plastic deformation; differential speed rolling; IF steel; structure; mechanical properties

Citation: Ko, Y.G.; Hamad, K. Development of Ultrafine Grain IF Steel via Differential Speed Rolling Technique. *Metals* **2021**, *11*, 1925. https://doi.org/10.3390/met11121925

Academic Editor: Andrey Belyakov

Received: 7 November 2021
Accepted: 26 November 2021
Published: 29 November 2021

1. Introduction

The metallic materials that have improved mechanical properties receive great attention, both in academic and industrial fields. For instance, steel has been regarded as a dominant material for numerous products since these materials possess unrivaled combinations of promising properties and low cost, making it affordable compared to the other materials. Among the various types of steel materials, IF (Interstitial-free) steel is widely used for automotive industries, due to its excellent processability and formability. The IF steel contains less than 0.01 wt.% carbon, leading to a fully ferritic microstructure; accordingly, it exhibits low strength and high ductility at room temperature. In this regard, its mechanical strength needs to be enhanced without a large decrease in ductility. This can be performed through a plastic deformation process where the structure is modified to reach the targeted properties.

For example, the strength of metals can be enhanced through grain refinement according to the Hall–Petch equation, and this can be achieved using severe plastic deformation (SPD) methods, such as equal channel angular pressing, high-pressure torsion, accumulative roll bonding, etc. [1–5]. However, due to their nature, the applicability of SPD methods is limited and cannot be used for large-scale production. Thus, to avoid this, asymmetrical rolling (ASR) has been found to be an effective technique by which the fine or ultrafine metals with high strength can be obtained in a larger scale [6–8]. Several reports on various metals produced via ASR show considerable results that the deformation, where the upper and lower roll speeds—hereafter called differential speed rolling (DSR) [4]—were set to be

different, was found to be very effective and reliable in producing metallic materials with improved properties [9–11]. Considering the promising properties of SPD-fabricated metals, the large-scale fabrication of metals using SPD methods is still a challenge, especially in the case of ECAP and HPT. Recently, a friction welding process was used to fabricate steel samples with an ultrafine-grained structure with optimized properties [12]. In this regard, due to its continuous nature, the DSR process can be used to fabricate metallic materials with ultrafine-grained structures in large scales.

Second, it was found that the textural change of the IF steels has a significant impact when determining the final properties, such as high deformability, since the grain reorientation would occur during deformation [13]. For instance, the texture development of {111}||ND, which is responsible for enhancing planar isotropic properties, could be produced by utilizing hot rolling [14,15]. At first, strong {111}||ND recrystallization textures in IF steel were evolved through a hot rolling operation, leading to a recrystallized microstructure. However, due to the difference in the composition between various IF steels, the microstructure, texture, and properties would be different—even in the same process. In addition, it was also reported that the texture developed during hot rolling was found to be inhomogeneous, influenced by the main texture components of the parent austenite [16]. In addition, the texture of the IF steel, which was evolved during cold rolling, was investigated too [17,18]. The γ-fiber ({111}||ND) was formed after cold rolling, with a reduction of 30%; then, the α-fiber (RD||<110>) appeared after cold rolling, with a reduction of 50%. The strengthening of the α-fiber is the main characteristic of the deformation, with 70% reduction. On the other hand, it was found that the distribution of plastic deformation imposed on the sample using conventional rolling was not uniform, resulting in the high heterogeneity in the texture formation throughout the sample [19].

In this study, DSR deformation will be used to modify the texture and microstructure of IF steel, and, as a result, the mechanical properties associated with the evolved structural parameters will be investigated. The dominated mechanism responsible for the grain refinement in IF steel, as it is induced by DSR deformation, will be investigated in this study too.

2. Experimental Procedure

The IF steel samples, in the form of sheets containing 0.009 wt.% C, were used in the present work. Figure 1 shows the initial microstructure of the IF steel sample with recrystallized grain structure (~35 μm). For the DSR deformation, the sheets were cut into small plates (90 mm × 30 mm × 4.8 mm). Then, the plates were subjected to 4 passes of DSR deformation at room temperature (RT), with a 30% reduction per pass, leading to a strain of ~0.43; a roll speed ratio of 1:4 (lower to upper rolls) was used in the deformation. The samples were flipped around 180 degrees to their longitudinal axis between each passage to control the materials with fine grains, which required the utilization of different shear characteristics during the DSR deformation. For ease of understanding, the schematic diagram of the DSR operation in this study is provided in Figure 2. Right after the RT DSR deformation, samples were prepared for structural characterizations and mechanical tests.

The microstructure characteristics were determined via both optical and transmission electron microscopy (TEM). The samples for TEM observations were first prepared through mechanical grinding and polishing to obtain foils with less than 0.1 mm in thickness, and then these foils were subjected to electropolishing using a 10% perchlorate solution. The TEM micrograph and diffraction from the selected area were performed using a TEM (model H-7600, Hitachi, Japan) machine with an acceleration voltage of 120 kV. Electron backscatter diffraction (EBSD) was employed to study the texture of the DSR-deformed samples; for this, a field emission scanning electron microscope (model S-4300SE, Hitachi, Japan) was used. Sample preparations for EBSD and the optical microscope (OM) were the same, where samples cut from the thickness direction (normal direction–rolling direction (ND–RD)) of the deformed plates were mechanically ground and polished. They were etched using a nital (nitric acid in methanol) solution.

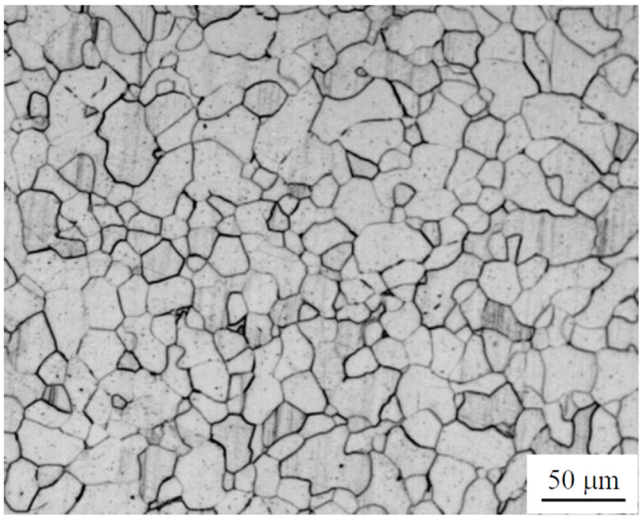

Figure 1. Initial microstructure of the IF steel sample used in the present work.

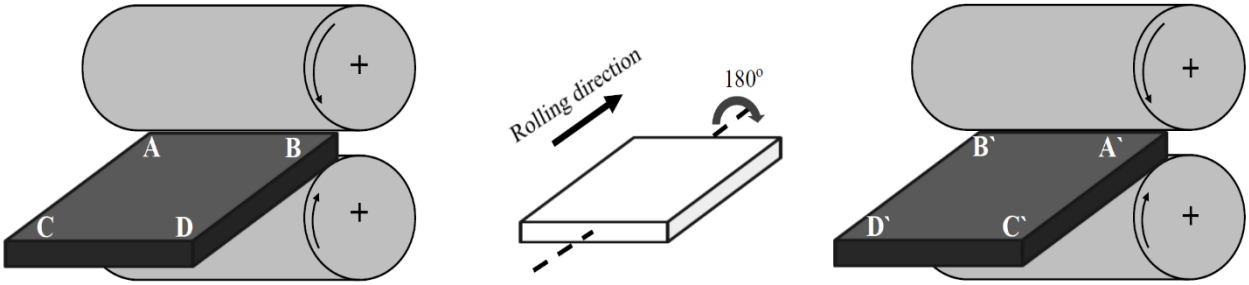

Figure 2. Differential speed rolling (DSR) technique used in the present work.

Some non-etched OM samples were used in the Vickers microhardness tests, which used the load and time of 0.1 Kg for 10 s, respectively. The hardness of the DSR-deformed samples was investigated throughout the thickness direction of the sample (the ND–RD plane), where indentation measurements (more than 20) were taken in various positions on this plane, and an average value was calculated. The standard deviation of these measurements can represent the homogeneity, where more deviation represents less homogeneity. Tensile tests were conducted at room temperature on samples (25 mm length, 4 mm width, and 1 mm thickness) cut from the plate after the DSR deformation. The crosshead of the tensile machine was set to obtain a strain rate of 10^{-3} s^{-1}.

3. Results and Discussion

3.1. DSR Deformation

Figure 3 displays the load–stroke curves during DSR deformation, with respect to the number of DSR operations. The loads of the IF steel samples were apt to rapidly increase, and reached a steady state as the materials were inserted into the rotated rolls. The curve also shows that the load for the deformation of the IF steel sheet sample was gradually increased with the increasing strain, where it slightly decreased after four operations of DSR. It was assumed that the increment of the load during deformation was attributed to strain hardening, while the significant microstructural change was contributed to the decrement of load. To fully understand those mechanisms, further observation in the microstructural analysis is provided.

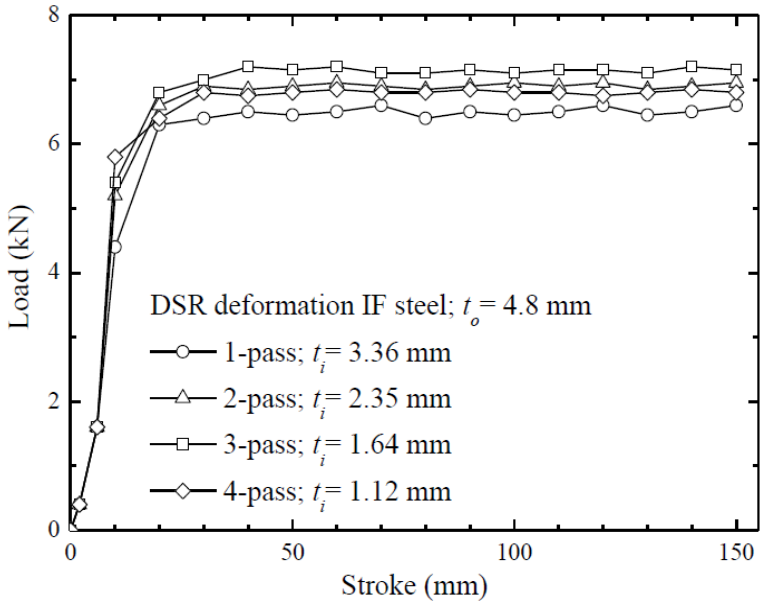

Figure 3. Load–stroke curves, recorded during the DSR deformation while the IF steel sample underwent the various processing conditions.

3.2. Microstructural Evolution

In the present study, the DSR-deformed IF steel samples have a good appearance without any cracking. Figure 4 shows the IQ (image quality) maps of the IF steel samples—taken along the thickness direction of these samples after one, two, three, and four passes of the DSR—and taken from the middle regions on the ND–RD planes.

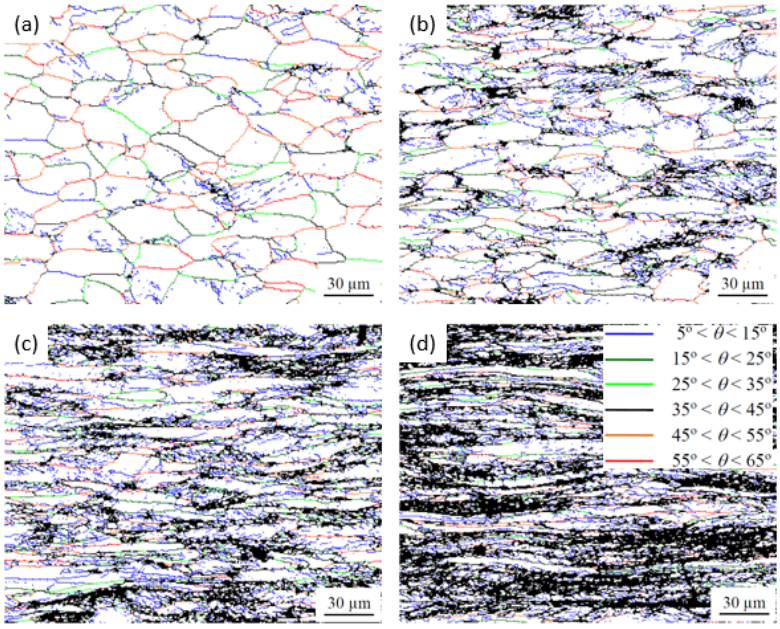

Figure 4. (**a**–**d**) Grain boundaries map of the IF steel samples deformed by 1, 2, 3, and 4 passes of DSR, respectively.

The evolution of the ferrite grains with misorientation bigger than 15° (high angle boundaries (HABs)) were tracked to see how the DSR processing modified the structure. After one pass of DSR, the microstructure of the deformed sample exhibited HABs parallel to the RD, forming elongated grains, as shown in Figure 4a. Due to the small amount of strain (~0.4) introduced into the sample, the structure seemed to be highly deformed but

with no indication of forming ultrafine grains. By increasing the introduced strain, the structure became more severely deformed after the fourth pass, which is equal to a strain of ~1.7; ultrafine grains were observable using the EBSD, as seen from Figure 4b–d, and these results were like those from previous investigations [20,21]. The microstructure showed relatively elongated grains with regular orientations along the rolling direction after the four-pass DSR deformation. In addition, the presence of the black color increased, indicating that the present microstructure contained high internal stress due to the severe plastic deformation imposed by the DSR; thus, the specific grain could not be detected during observation. Furthermore, the microstructures exhibited evidence of the homogeneous penetration of shear strain throughout the thickness of the DSR-deformed IF steel sample, where this was indicated by the general shape of the grain being severely elongated and parallel to the deformation flow.

To figure out the general microstructural trends, EBSD analyses on hundreds of deformed grains were conducted to measure the grain size and misorientation distributions, as seen from Figure 5. In Figure 5a, the grain size distribution of the IF steel deformed by a single DSR was dominated by a coarse ferrite grain of ~14 μm. After two-pass DSR deformation, the grain size distribution became relatively narrow, obtaining the mean size of ~8 μm. When increasing the amount of strain, the UFG structure with an average size of ~0.7 μm was obtained after the four-pass DSR deformation due to the accumulation of plastic deformation that was stored during multi-pass processing. Figure 5b shows the distribution of the grain misorientation angle of the deformed microstructure during DSR. After the single DSR deformation, most of the grain boundaries of the deformed microstructure possessed a low angle misorientation, and a small fraction of high angle grain boundaries (HAGBs, 15° or higher) were detected (as low as ≈25%). After two passes, the volume fraction of HAGBs slightly increased, implying that the number of lattice dislocations due to repetitive DSR deformation was absorbed by subgrain boundaries, which led to the transformation of grain boundaries from low angle to high angle characteristics [22,23]. After the four pass DSR, the deformed IF steel showed a noticeable increase in the volume fraction of HAGBs up to ≈58%.

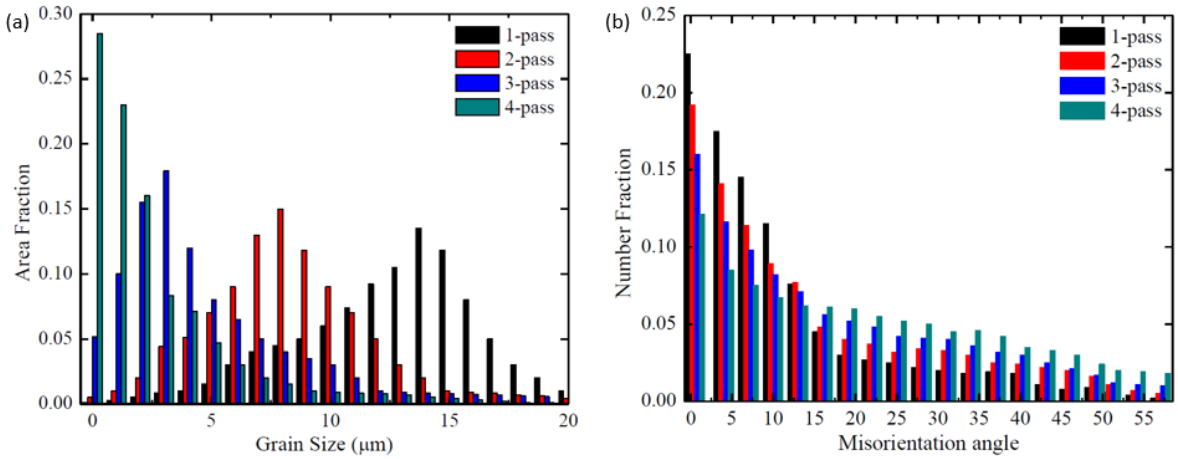

Figure 5. (**a**) Grain size and (**b**) grain boundary characteristics of the IF steel samples, respectively, deformed by DSR under the various conditions.

A close examination, as displayed in Figure 6a–d and obtained using TEM, shows the important features of the microstructure of the deformed samples where the grain was successfully refined to ~0.7 μm. It is apparent that most of the grains were considerably equiaxed after two and four passes of DSR, as seen in Figure 6b,d. The formation of the nearly equiaxed grains could be explained by modifying the shearing characteristics affected by the deformation route associated with the sample rotation of each passage. The deformation of the sample rotating 180 degrees around its longitudinal axis results

in macroscopic intersecting shearing. Hence, the dislocation slip would conjugated at each even-numbered pass, allowing the subgrains to restore their original segments in order to accommodate severe plastic deformation. Furthermore, the selected area's electron diffraction pattern in the DSR-deformed IF steel sample revealed a ring-like pattern, as shown in Figure 6d, which confirmed the formation of an ultrafine grain structure.

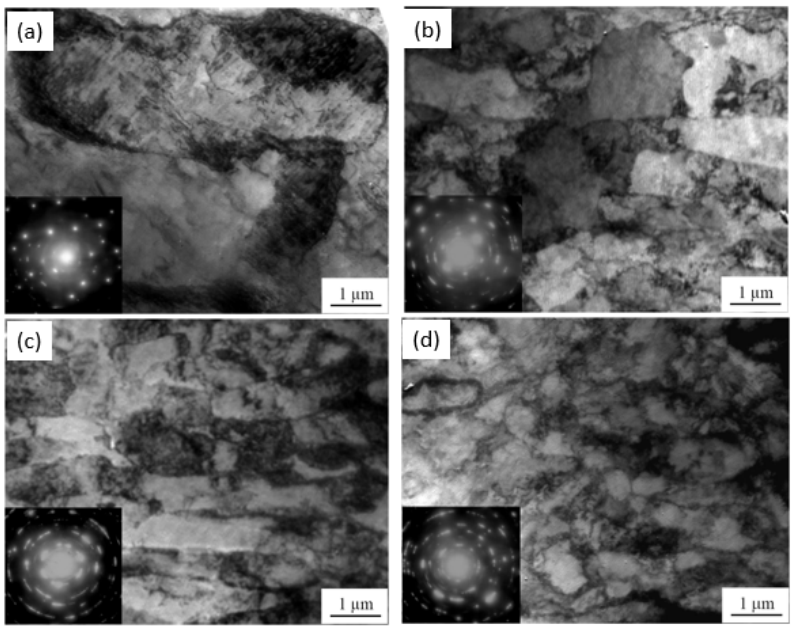

Figure 6. (**a**–**d**) TEM and selected area diffraction of the IF steel samples, deformed by 1, 2, 3, and 4 passes of DSR, respectively.

3.3. Textural Evolution

Figure 7 shows the (110) pole figure of the deformed sample with respect to DSR. After one pass of DSR, the α-fiber of the {112} <110> slip was found to be the dominant slip system for accommodating the plastic strain in the deformed IF steel samples. Both α-fibers remained constant as a dominant slip and intensified even after four passes of DSR deformation. In addition, it was found that the γ-fiber of {111} <112>, which is responsible for good deformability, was activated after four operations of DSR deformation.

Figure 8 depicts the bulk texture evolution, which is indicated by Φ_2 = 45° ODF sections of the DSR-deformed IF steel samples with respect to the number of passes. During DSR deformation, the ε-fiber of {001}||ND was constantly activated as the strain increased, even its intensity was increased after four passes of DSR deformation. In γ-fiber evolution, the {111} <110> and {111} <1–21> slips were activated after one pass of DSR deformation. Then, it rotated to the {111} <112> slip, which is the strongest component among the γ-fiber, after two and three passes. After four passes of DSR deformation, the {111} <112> slip partly shifted to {111} <0–11>. In addition, the intensity γ-fiber strengthened with the increasing strain. For α-fibers' evolution, the {001} <100> and {112} <110> slips were activated after one pass of DSR, and its intensity was increased up to three passes of DSR deformation. Nevertheless, their intensities slightly reduced after four passes of DSR, which might be attributed to the crystal shifting to γ-fiber of {111} <211>. Thus, according to these results, the crystal rotations during DSR deformation occurred along two paths: (i) {001} <110> $\rightarrow$ {112} <110> $\rightarrow$ {111} <112> and (ii) {111} <1–21> $\rightarrow$ {111} <112> $\rightarrow$ {111} <0–11>. Clearly, the rotations along both paths seem plausible in explaining the textural change of the present work.

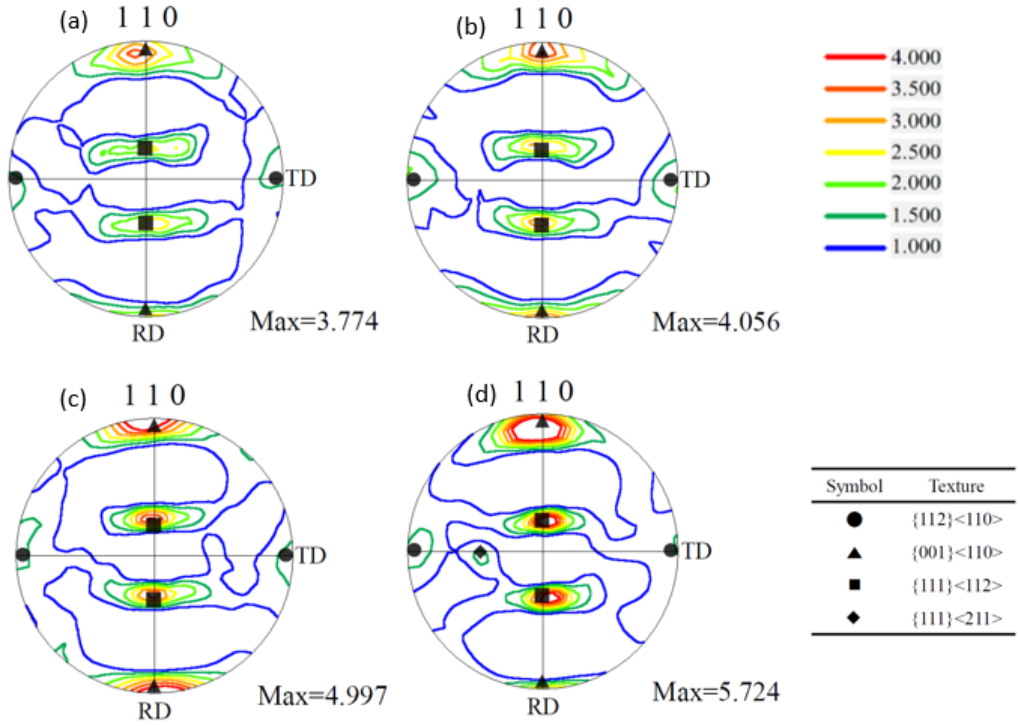

Figure 7. (**a**–**d**) Pole figures of the IF steel samples, deformed by 1, 2, 3, and 4 passes of DSR, respectively.

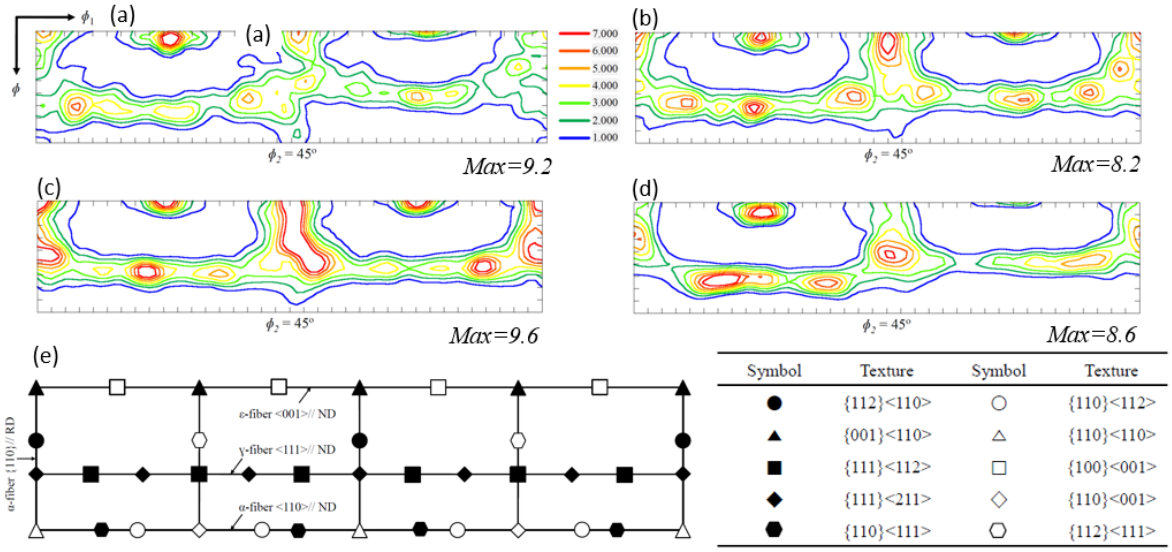

Figure 8. (**a**–**d**) Orientation distribution functions of the IF steel samples, deformed by DSR under various conditions. (**e**) The texture components of BCC metals.

3.4. Mechanical Responses

Figure 9 shows the microhardness results of the DSR-deformed samples under the various processing conditions. The results show that the hardness values increased by a factor of 2.5—that is, from ~98 in the non-deformed sample to ~235 Hv in the four pass DSR-deformed sample, with the tendency of the value to increase significantly after the first pass and modestly during subsequent DSR deformation. This hardening can be attributed to the dislocation accumulation effect (work hardening) and the grain size reduction (Hall–Petch strengthening) [24], leading to a significant improvement in the strength after the DSR deformation as compared to the non-deformed sample.

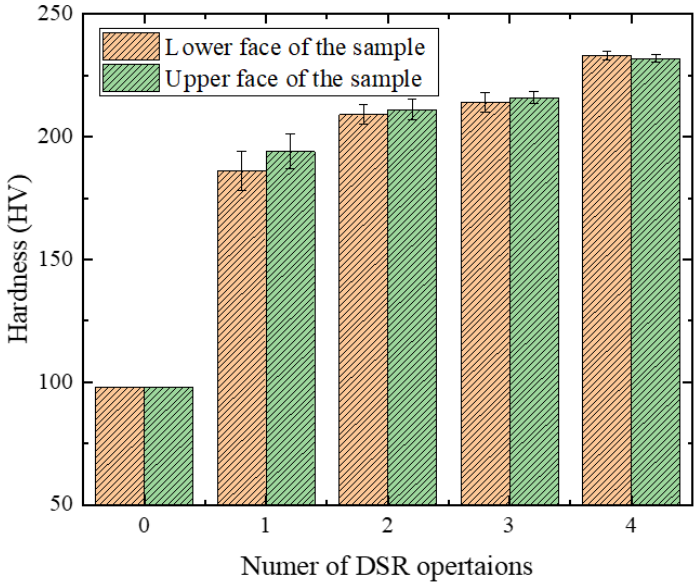

Figure 9. Microhardness measurements of the IF steel samples, deformed by DSR under various conditions.

In addition, it is worth noting that the hardness values measured in the counterpart faces of the sample became closer to each other by increasing the number of DSR passes. This trend is mainly attributed to the deformation path used in the present work. In this path, the sample was rotated by 180 degrees around its rolling direction between the successive passes; accordingly, the deformation can be introduced homogeneously through the sample, leading to uniform hardness after the four-pass DSR. The related illustration is also provided in Figure 10.

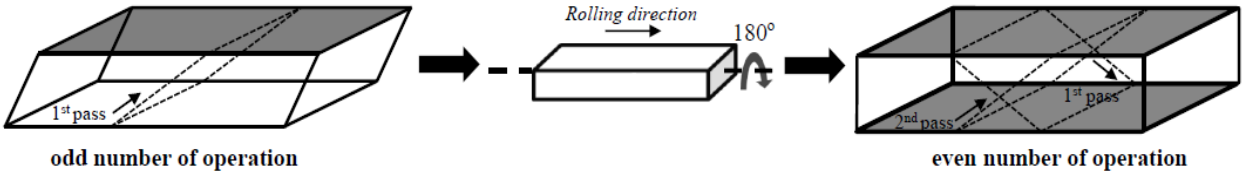

Figure 10. DSR route used in the present work, showing the interaction of the shear band during the deformation.

Figure 11 shows the room temperature tensile curves of the steel samples after the DSR deformation under the various conditions. The tensile properties of the DSR-deformed samples, including yield strength (YS), ultimate tensile strength (UTS), and elongation at break are presented in Table 1. It is clearly seen from Figure 11 and the properties listed in Table 1 that the strength (both the YS and UTS) increases by increasing the amount of deformation introduced by the DSR process, and this was entirely consistent with the trend noted in the hardness results. Here, a maximum UTS of 0.78 GPa was reached by the four-pass DSR processing. Based on the structural evolution discussed in the above sections, one can clearly attribute the strengthening to the Hall–Petch (grain size), where the fraction of HAGs increased sharply by increasing the number of DSR passes. This suggests the evolution of a higher number of ultrafine grains (Figure 5b). In addition, the ductility of the DSRed samples was reduced by increasing the amount of introduced deformation, where a ductility of 7.8% was reached in the four-pass sample, and this value was a little higher than that obtained in the three-pass sample. This can be attributed to the stronger shear texture evolved in the four-pass sample as compared to others. In addition, this softening in the four-pass DSR sample could be the reason behind the decrease in the load during the deformation, as seen by Figure 3.

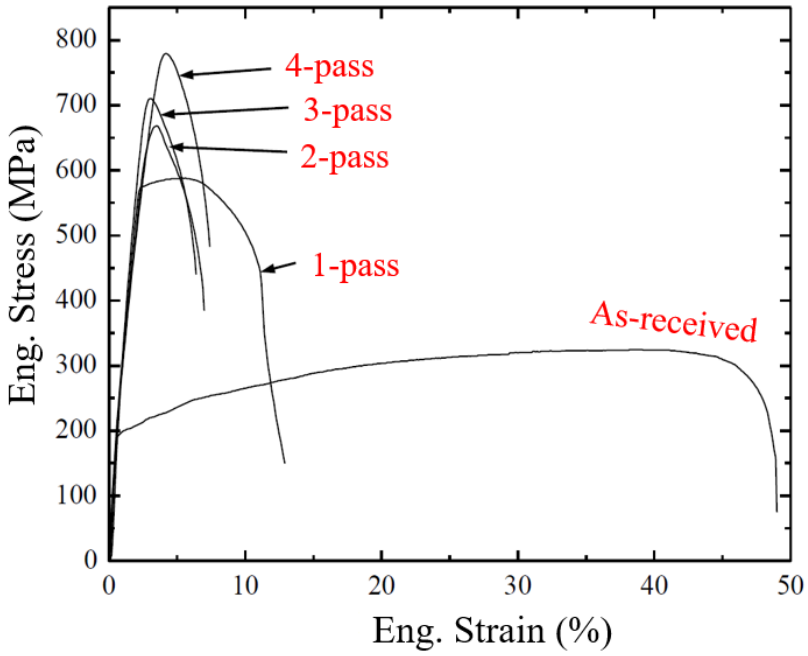

Figure 11. Room temperature tensile curves of the IF steel samples, deformed by DSR under various conditions.

Table 1. Mechanical properties of ultrafine-grained IF steel samples.

Sample	YS (MPa)	UTS (MPa)	Elongation (%)	Yield Ratio *	Microhardness
As-received	207	430	56	0.48	98
1 pass	566 ± 23	587 ± 19	12.9 ± 2	0.96	192
2 pass	613 ± 31	668 ± 22	7 ± 1.2	0.91	211
3 pass	667 ± 19	710 ± 36	6.4 ± 2.2	0.93	217
4 pass	770 ± 26	780 ± 28	7.4 ± 1.5	0.98	235

* Yield ratio = yield strength/ultimate tensile strength.

4. Conclusions

In the present work, IF steel samples were plastically deformed using the DSR method to modify the structure and improve the mechanical properties of these samples. The following conclusions can be reached from this work:

1. The DSR process can be successfully used to deform metallic materials plastically.
2. An ultrafine structure, with a grain size of less than 1 μm, was evolved after the DSR deformation, and those grains are surrounded by high-angle grain boundaries.
3. Strong shear texture components were recorded for the IF steel sample deformed by four passes of DSR.
4. As a result of grain refinement induced by the deformation, the strength (YS and UTS) and hardness of the deformed IF steel samples increased by increasing the number of DSR passes.
5. The ductility decreased in the IF steel samples by increasing the number of DSR passes.

Author Contributions: K.H. Investigation, Formal analysis, Data curation, Visualization, Writing—original draft, Funding acquisition. Y.G.K. Supervision, Conceptualization, Writing—review & editing. All authors have read and agreed to the published version of the manuscript.

Funding: This research was funded by National Research Foundation (NRF) of South Korea, grant number (2020R1A2C1004720). And the APC was funded by National Research Foundation (NRF) of South Korea, grant number (2020R1A2C1004720).

Data Availability Statement: Not applicable.

Acknowledgments: This research was supported by the National Research Foundation (NRF) of South Korea (2020R1A2C1004720).

Conflicts of Interest: The authors declare no conflict of interest.

References

1. Zhou, T.; Guo, F.; Zhang, Q.; Liu, D. Offsetting strength-ductility tradeoff in Mg-Sn-Zn-Zr alloy by a novel differential-thermal ECAP process. *Mater. Lett.* **2021**, *305*, 30764. [CrossRef]
2. Kalahroudi, J.; Koohdar, H.; Langdon, T.G.; Ahmadabadi, M. Phase evolution and mechanical properties of an intercritically-annealed Fe–10Ni–7Mn (wt.%) martensitic steel severely deformed by high-pressure torsion. *Mater. Sci. Eng. A* **2021**, *804*, 140519. [CrossRef]
3. Ko, Y.G.; Hamad, K. Annealing characteristics of ultrafine grained low-carbon steel processed by differential speed rolling method. *Metall. Mater. Trans. A* **2016**, *47*, 2319.
4. Hamad, K.; Ko, Y.G. Continuous differential speed rolling for grain refinement of metals: Processing, microstructure, and properties. *Solid State Mater. Sci.* **2019**, *44*, 470. [CrossRef]
5. Azushima, A.; Kopp, R.; Korhonen, A.; Yang, D.Y.; Micari, F.; Lahoti, G.D.; Groche, P.; Yanagimoto, J.; Tsuji, N.; Rosochowski, A.; et al. Severe plastic deformation (SPD) processes for metals. *CIRP Ann.-Manuf. Technol.* **2008**, *57*, 716. [CrossRef]
6. Cui, Q.; Ohori, K. Grain refinement of high purity aluminium by asymmetric rolling. *Mater. Sci. Technol.* **2000**, *12*, 1095. [CrossRef]
7. Lee, J.B.; Konno, T.J.; Jeong, H.G. Grain refinement and texture evolution in AZ31 Mg alloys sheet processed by differential speed rolling. *Mater. Sci. Eng. B* **2009**, *161*, 166. [CrossRef]
8. Sidor, J.; Miroux, A.; Petrov, R.; Kestens, L. Microstructural and crystallographic aspects of conventional and asymmetric rolling processes. *Acta Mater.* **2008**, *56*, 2495. [CrossRef]
9. Kim, W.J.; Hwang, B.G.; Lee, M.J.; Park, Y.B. Effect of speed-ratio on microstructure, and mechanical properties of Mg–3Al–1Zn alloy, in differential speed rolling. *J. Alloys Compd.* **2011**, *509*, 8510. [CrossRef]
10. Kim, W.J.; Lee, H.W.; Yoo, S.J.; Park, Y.B. Texture and mechanical properties of ultrafine-grained Mg–3Al–1Zn alloy sheets prepared by high-ratio differential speed rolling. *Mater. Sci. Eng. A* **2011**, *528*, 874–879. [CrossRef]
11. Ko, Y.G.; Kim, Y.G.; Hamad, K. Microstructure optimization of low-carbon steel using differential speed rolling deformation followed by annealing. *Mater. Lett.* **2020**, *261*, 127154. [CrossRef]
12. Skowrońska, B.; Chmielewski, T.; Pachla, W.; Kulczyk, M.; Skiba, J.; Presz, W. Friction Weldability of UFG 316l Stainless SteeL. *Arch. Metall. Mater.* **2019**, *64*, 1051.
13. Tóth, L.S.; Jonas, J.J.; Daniel, D.; Ray, R.K. Modeling of rolling texture development in a ferritic chromium steel. *Metall Trans. A* **1990**, *21*, 2985. [CrossRef]
14. Ghosh, P.; Ghosh, C.; Ray, R.K. Thermodynamics of precipitation and textural development in batch-annealed interstitial-free high-strength steels. *Acta Mater.* **2010**, *58*, 3842. [CrossRef]
15. Khatirkar, R.K.; Kumar, S. Comparison of recrystallization textures in interstitial free and interstitial free high strength steels. *Mater. Chem. Phys.* **2011**, *127*, 128. [CrossRef]
16. Cheng, G.; Gault, B.; Huang, C.; Huang, C.; Yen, H. Warm ductility enhanced by austenite reversion in ultrafine-grained duplex steel. *Acta Mater.* **2018**, *148*, 344. [CrossRef]
17. Li, J.X.; Liu, Z.Y.; Gao, C.; Wang, Z.D.; Liu, X.H.; Wang, G.D. Evolution of textures in interstitial free steel during multiple cold rolling and annealing. *J. Mater. Proc.* **2005**, *167*, 132.
18. Li, B.L.; Godfrey, A.; Meng, Q.C.; Liu, Q.; Hansen, N. Evolution of microstructure and local crystallographic orientations in rolled Al–1%Mn single crystals of {0 0 1}<110> orientation. *Acta Mater.* **2004**, *52*, 1069. [CrossRef]
19. Lee, S.H.; Lee, D.N. Analysis of deformation textures of asymmetrically rolled steel sheets. *Int. J. Mech. Sci.* **2001**, *43*, 1997. [CrossRef]
20. Wauthier, A.; Réglé, H.; Brenner, R. Evolution of the Deformed Substructure Obtained by Cold-Rolling in IF Steel. *Mater. Sci. Forum* **2007**, *550*, 205. [CrossRef]
21. Hamad, K.; Ko, Y.G. Effect of roll speed ratio on microstructure evolution and mechanical properties of 0.18 wt% carbon steel deformed by differential speed rolling. *Mater. Lett.* **2015**, *130*, 213. [CrossRef]
22. Dougherty, L.M.; Robertson, I.M.; Vetrano, J.S. Direct observation of the behavior of grain boundaries during continuous dynamic recrystallization in an Al–4Mg–0.3Sc alloy. *Acta Mater.* **2003**, *51*, 4367. [CrossRef]
23. Chang, L.L.; Cho, J.H.; Kang, S.B. Microstructure and mechanical properties of AM31 magnesium alloys processed by differential speed rolling. *J. Mater. Process Technol.* **2011**, *211*, 1527. [CrossRef]
24. Ding, Y.; Jiang, J.; Shan, A. Microstructures and mechanical properties of commercial purity iron processed by asymmetric rolling. *Mater. Sci. Eng. A* **2009**, *509*, 76. [CrossRef]